

ROTATIONAL SPECTRA OF THE CARBON CHAIN NEGATIVE IONS C_4H^- AND C_8H^-

H. GUPTA,^{1,2} S. BRÜNKEN,¹ F. TAMASSIA,³ C. A. GOTTLIEB,¹ M. C. MCCARTHY,¹ AND P. THADDEUS¹

Received 2006 November 1; accepted 2006 December 12; published 2007 January 11

ABSTRACT

The rotational spectra of the butadiyne anion C_4H^- and the octatetrayne anion C_8H^- have been detected in the laboratory. Precise spectroscopic constants for these closed-shell molecules have been obtained, which enable their rotational spectra to be calculated to high accuracy throughout the radio band. Deep astronomical searches can now be undertaken in essentially any molecular source, including TMC-1 and IRC +10216, where the negative ion C_6H^- has recently been detected. The large dipole moments and high binding energies of both anions make them good candidates for astronomical detection.

Subject headings: ISM: molecules — line: identification — molecular data — molecular processes — radio lines: ISM

We recently detected the radio spectrum of the negative ion C_6H^- in the laboratory and showed that this surprisingly large carbon chain anion is the carrier of the unidentified harmonic sequence of molecular lines B1377 observed by Kawaguchi et al. (1995) in the circumstellar shell of the carbon star IRC +10216 (McCarthy et al. 2006). The radio spectra of other molecular anions should now be detectable in the laboratory and in space, especially linear closed-shell carbon chains similar in structure to C_6H^- . Here we report laboratory detection of the next shorter and the next longer members of the series, the butadiyne anion C_4H^- and the octatetrayne anion C_8H^- . Precise transition frequencies over most of the radio band are now available for astronomical searches for these anions.

Like C_6H^- , the C_4H^- anion has been observed in both the millimeter-wave band with a free space (FS) spectrometer (Gottlieb et al. 2003) and the centimeter-wave band with a Fourier transform microwave (FTM) spectrometer (McCarthy et al. 2000). The longer anion C_8H^- has only been detected with the highly sensitive FTM instrument, since its rotational lines are fairly weak. Seventeen rotational transitions between 9 and 363 GHz of C_4H^- and nine successive rotational transitions between 9 and 19 GHz of C_8H^- have been measured to an accuracy approaching 1 part in 10^7 (see Tables 1 and 2).

In the FS spectrometer, C_4H^- was produced by a DC glow discharge through a flowing mixture of argon (15%) and acetylene (85%) at a total pressure of ≤ 10 mtorr with the discharge cell walls cooled to 100 K. As with C_6H^- , the optimum discharge current (~ 150 mA) was substantially lower than that which produces the most intense lines of the neutral radical (~ 400 mA). At this lower current, lines of C_4H^- were only about 8 times weaker than those of either fine-structure component of C_4H ; hyperfine structure of C_4H collapses at high J and is not resolved at millimeter wavelengths, but spin-doubling does not collapse and is resolved. Taking the different partition functions and dipole moments into account, the abundance of the anion is found to be $\sim 0.14\%$ that of the neutral. The $J = 37 \leftarrow 36$ absorption line of C_4H^- is shown in Figure 1; a signal-to-noise ratio of ~ 75

was obtained in only 25 minutes of integration, allowing line frequencies to be measured to 10–20 kHz.

In the FTM spectrometer, the anions were produced under discharge conditions similar to those in which C_6H^- is observed: a 600–700 V low-current (10–20 mA) DC discharge, a gas pulse 300 μ s long (for a flow of 20–25 $\text{cm}^3 \text{ minute}^{-1}$ at STP), the precursor gas consisting of diacetylene (0.1%) heavily diluted with an inert buffer gas (Ne, He, or H_2) at a stagnation pressure of 2.5 ktorr behind the pulsed valve of the nozzle. The cavity mirrors and first-stage amplifier were cooled to 77 K to reduce thermal noise. Lines of C_4D^- and C_8D^- were detected in a discharge through deuterated diacetylene. As before, the polarity of the discharge is important in the production of the anions, which are best observed with the polarity reversed with respect to that which produces the neutrals (Taylor et al. 1998). The abundance of C_4H^- relative to C_4H depended on the buffer gas, ranging from 1.2×10^{-3} with H_2 to an upper limit of 4×10^{-5} with Ne—considerably lower than the ratio of C_6H^- relative to C_6H . Under the best conditions, the strongest lines of C_8H^- were observed with a signal-to-noise ratio of 10 in 90 minutes of integration (see Fig. 2). The lines of C_8H^- are about 10% as strong as those of the neutral radical observed under the same conditions but are only a factor of 2–3 weaker than those of C_6H^- . We estimate that there are $\sim 10^8$ C_8H^- molecules per gas pulse (by comparison with lines obtained with a calibrated sample of 1% OCS in Ne), which corresponds to about 2% that of C_8H —a similar ratio to that found for C_6H^- relative to C_6H .

The searches for the two anions here were guided by high-level ab initio molecular structure calculations [at the CCSD(T)/cc-pVTZ level of theory]. Precise equilibrium structures were obtained and then corrected for vibrational effects (see Table 3 note). All calculations were performed with the ACES II suite of programs (Stanton et al. 1992). The theoretical ground-state rotational constants are summarized in Table 3. For C_4H^- the calculated rotational constant agrees well with that obtained by photodetachment spectroscopy of the rotationally resolved ${}^1A' \leftarrow X {}^1\Sigma^+$ electronic transition ($B = 4653 \pm 6$ MHz; Pachkov et al. 2003) and a previous high-level theoretical calculation ($B = 4658$ MHz; Botschwina 2000). The initial search for C_4H^- in the millimeter-wave band covered a frequency range of $\pm 0.15\%$ for three successive transitions ($J = 18 \leftarrow 17$, $19 \leftarrow 18$, and $20 \leftarrow 19$). A single harmonic series of lines of comparable strength was found, and the search was then extended to detect additional lines in narrowband scans close to the fre-

¹ Harvard-Smithsonian Center for Astrophysics, Cambridge, MA; and Division of Engineering and Applied Sciences, Harvard University, Cambridge, MA; hgupta@cfa.harvard.edu, sbrunken@cfa.harvard.edu, cgottlieb@cfa.harvard.edu, mccarthy@cfa.harvard.edu, pthaddeus@cfa.harvard.edu.

² Also at Institute for Theoretical Chemistry, Department of Chemistry and Biochemistry, The University of Texas, Austin, TX.

³ Dipartimento di Chimica Fisica e Inorganica, Università di Bologna, Bologna, Italy; tamassia@ms.fci.unibo.it.

TABLE 1
LABORATORY ROTATIONAL FREQUENCIES OF C_4H^-

$J' - J''$	Frequency (MHz)	$O - C^a$ (kHz)
1-0	9,309.887	-2
2-1	18,619.758	-3
9-8	83,787.263	-33
16-15	148,948.610	-3
17-16	158,256.620	37
18-17	167,564.324	11
19-18	176,871.783	-6
20-19	186,179.030	33
26-25	242,015.829	0
27-26	251,320.800	33
28-27	260,625.328	4
29-28	269,929.465	-21
31-30	288,536.554	-15
32-31	297,839.465	3
37-36	344,346.858	-16
38-37	353,646.854	6
39-38	362,946.288	3

NOTE.—Estimated 1σ uncertainties in the line frequencies: 2 kHz in the two lowest transitions, 15 kHz in the millimeter-wave transitions.

^a Calculated from the spectroscopic constants in Table 3.

quencies predicted on the basis of this limited data set. The search for C_8H^- in the centimeter-wave region was similar. The spectroscopic constants of both species are given in Table 3.

The evidence that the lines are from C_4H^- and C_8H^- is extremely strong. The derived rotational constants B are within 0.1% of those calculated ab initio, and the small ratios of the centrifugal distortion constant to the rotational constant ($D/B = 1.3 \times 10^{-7}$ and 7×10^{-9} , respectively) are characteristic of linear carbon chains (Gottlieb et al. 1983; McCarthy et al. 1999). In addition, the rotational spectra of the deuterated species were obtained at the expected isotopic shifts (7.1% and 3.3%, respectively) to better than 0.05%. The absence of fine and hyperfine structure in the high-resolution FTM measurements (line width 10–20 kHz) and the closely harmonic sequence of the lines strongly indicate closed-shell linear molecules with $^1\Sigma^+$ ground states, as predicted (Pan et al. 2003; Pino et al. 2002).

As a further check, for C_4H^- we determined the charge of the carrier by measuring the rest frequency of individual rotational lines in single pass absorption in the FS spectrometer. As expected, Doppler shifts in the line frequencies are observed when the polarity of the discharge is reversed (owing to the axial drift of the ion; see Fig. 3), indicating a charged carrier. The sign of the shift is opposite to that observed for HCO^+ , confirming that the carrier is a negative ion.

From the spectroscopic constants derived here, rotational tran-

TABLE 2
LABORATORY ROTATIONAL FREQUENCIES OF C_8H^-

$J' - J''$	Frequency (MHz)	$O - C^a$ (kHz)
8-7	9,333.434	1
9-8	10,500.110	0
10-9	11,666.785	-1
11-10	12,833.460	0
12-11	14,000.134	0
13-12	15,166.806	0
14-13	16,333.476	-1
15-14	17,500.147	1
16-15	18,666.814	0

NOTE.—Estimated 1σ uncertainties in the line frequencies are 2 kHz.

^a Calculated from the spectroscopic constants in Table 3.

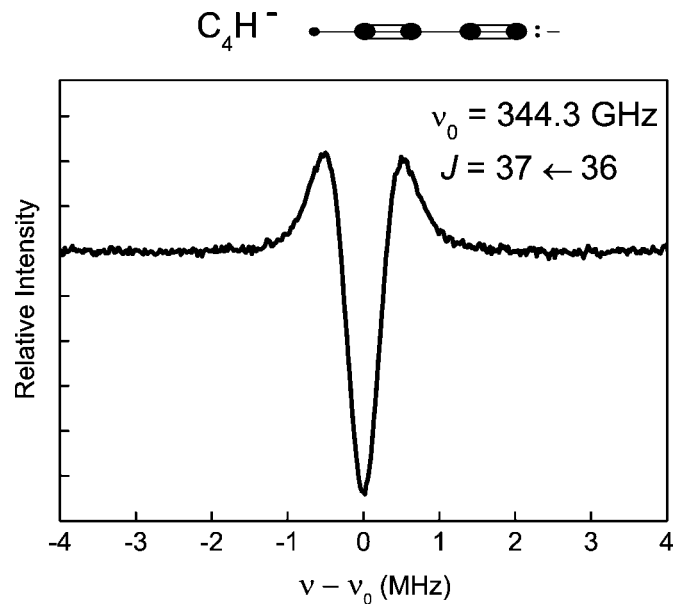


FIG. 1.— $J = 37 \leftarrow 36$ transition of C_4H^- observed with the free space millimeter-wave spectrometer, in an integration time of 25 minutes. Owing to the modulation scheme employed, the instrumental line shape is approximately the second derivative of a Lorentzian.

sitions of C_4H^- can now be predicted to better than 250 kHz or 0.1 km s^{-1} in equivalent radial velocity through 800 GHz. For C_8H^- , although the rotational and centrifugal distortion constants in Table 3 are derived from measurements below 19 GHz, they are so accurately determined that the radio spectrum of C_8H^- can now be calculated well beyond the range of measurement. For example, the uncertainty in equivalent radial velocity is less than 0.03 km s^{-1} at 20 GHz, and 0.4 km s^{-1} at 50 GHz—less than the line width in both TMC-1 and IRC +10216 at frequencies where C_8H has been found. We conclude that the predicted frequencies for both species are adequate for deep astronomical searches in all the standard molecular sources. At a

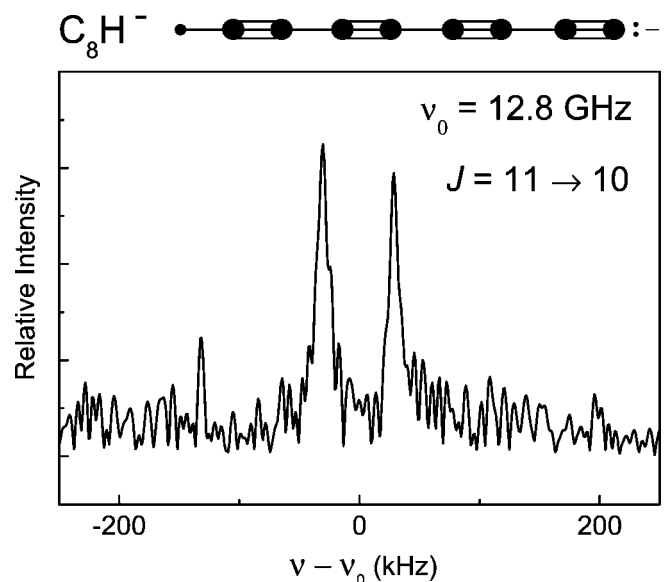


FIG. 2.— $J = 11 \rightarrow 10$ transition of C_8H^- observed with the FTM spectrometer—a 90 minute integration. The double-peaked instrumental line shape is caused by the Doppler shift of the supersonic molecular beam relative to the two traveling waves that compose the confocal mode of the Fabry-Perot cavity; the rest frequency of the transition is the average of these two components.

TABLE 3
SPECTROSCOPIC CONSTANTS OF C_4H^- AND C_8H^-

Constant	Laboratory	Theoretical
C_4H^-		
B	4654.9449(2)	4653.9 ^a
10^3D	0.5875(1)	0.55 ^b
C_8H^-		
B	583.34014(8)	583.2 ^a
10^6D	4.3(2)	3.5 ^c

NOTE.—Units are MHz.

^a B_e from a CCSD(T)/cc-pVTZ calculation. The vibration-rotation correction was calculated at the CCSD(T)/cc-pVDZ level of theory for C_4H^- , and the SCF/DZP level for C_8H^- .

^b From a CCSD(T)/cc-pVTZ calculation.

^c From a SCF/DZP calculation.

typical cold cloud temperature of 5 K, strong transitions of C_4H^- are expected from the centimeter-wave band below 50 GHz through the 3 mm wavelength region. At the slightly higher temperatures of 30–40 K found for carbon chain molecules in IRC +10216, the intensity peaks near 150 GHz. For C_8H^- the maximum in intensity lies in the centimeter-wave band in both cases. These frequency regions are all readily accessible with present large radio telescopes.

The ground states of both C_4H^- and C_8H^- have been predicted from ab initio calculations and photodetachment experiments to be $^1\Sigma^+$ (Pan et al. 2003; Pino et al. 2002). The expected rotational spectra therefore are those of simple linear molecules, devoid of the fine and hyperfine structure that is present in the neutral radicals, which possess $^2\Sigma^+$ or $^2\Pi$ ground states. This collapse of substructure alone results in a gain of 4–8 in intensity for individual lines of the anion relative to those of the neutral. Furthermore, our high-level ab initio calculations indicate that the dipole moments of the anions are significantly larger than those of the neutrals (6 D vs. 0.87 D for the four-carbon chain [Woon 1995] and 11.9 D vs. 6.3 D for the eight-carbon chain [McCarthy et al. 1996]), so that lines of the anion relative to those of the neutral are enhanced by 1–2 orders of magnitude or more—an effect that greatly benefits detection in the radio band.

We have failed to find lines of C_4H^- in the available astronomical line surveys of TMC-1 and IRC +10216. In TMC-1, a rotational temperature of ~ 5 K and a column density of $N = (0.3\text{--}1.3) \times 10^{15} \text{ cm}^{-2}$ were found for neutral C_4H (Guélin et al. 1982; Bell et al. 1983). The strongest predicted C_4H^- line ($J = 5 \leftarrow 4$) in the bandwidth of the 8.8–50 GHz survey with the Nobeyama 45 m telescope (Kaifu et al. 2004) toward this source is ≤ 20 mK. Assuming an excitation temperature of 5 K, this yields an upper limit for the C_4H^- column density of $N = 2.2 \times 10^{10} \text{ cm}^{-2}$, which is a factor of $(1\text{--}6) \times 10^4$ lower than that of the neutral. In IRC +10216, the C_4H radical has been detected with a column density of $N = (2.4\text{--}3.0) \times 10^{15} \text{ cm}^{-2}$ and an excitation temperature of 15–35 K, both in the centimeter-wave band (28–50 GHz; Kawaguchi et al. 1995) and the 2 mm wavelength region (129–172.5 GHz; Cernicharo et al. 2000). No lines of C_4H^- were found in either survey; on the assumption of an excitation temperature of 35 K, an upper limit is obtained for the C_4H^- column density of $N = 2 \times 10^{12} \text{ cm}^{-2}$, or 0.1% that of C_4H .

The upper limit for the anion-to-neutral ratio of C_4H derived both in the laboratory and toward the two astronomical sources IRC +10216 and TMC-1 is surprisingly low, more than an order of magnitude lower than that found for the longer chain

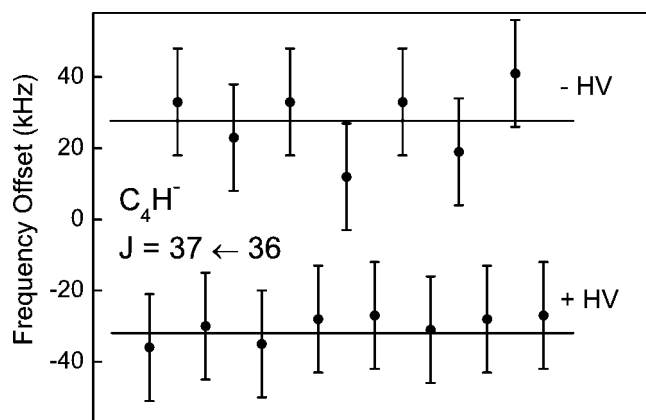


FIG. 3.—Ion drift measurements of C_4H^- . Plotted are a series of measurements of the $J = 37 \leftarrow 36$ line with either positive or negative high voltage (HV) applied to the electrode near the radiation source; the electrode on the detector side was at ground potential in either case. The frequency shift (relative to a center frequency of 344,346.874 MHz) corresponds to a drift velocity of 25 m s^{-1} .

C_6H . This low ratio may indicate anion formation from the neutral molecule by radiative electron attachment, a process that tends to become more efficient with increasing molecular size, i.e., a larger density of states, and a higher electron affinity, which promote electron capture and a faster relaxation to the anionic ground state. As predicted from a statistical approach by Terzieva & Herbst (2000) for pure carbon chain molecules, a critical size of about six carbon atoms is needed for efficient electron attachment, and the reaction rate is found to be an order of magnitude lower for smaller chains, which may explain the observed low abundance of C_4H^- in space. There may be other factors affecting the formation rate of hydrocarbon anions, in particular the role of intermediate dipole-bound states in electron capture. As discussed by Pachkov et al. (2003) a dipole-bound state is probably not formed from the ground state of C_4H , as it is for the longer chains, but rather from the low-lying $^2\Pi$ excited electronic state, which may be poorly populated in cold interstellar and circumstellar clouds. Detection of C_4H^- as a function of temperature, density, and extinction is probably required to understand the formation of this anion in space.

Similarly, we tried without success to find C_8H^- in existing astronomical surveys of IRC +10216, specifically in the 45 m Nobeyama survey by Kawaguchi et al. (1995), where the harmonic lines of C_6H^- were found. There are 16 rotational transitions of C_8H^- within the 22 GHz covered by the Nobeyama survey between 28 and 50 GHz, from $J = 28 \rightarrow 27$ to $43 \rightarrow 42$, the first about 23 K above the $J = 0$ ground state and the last about 53 K—fairly close to the maximum in the Boltzmann distribution. A reasonable limit on the peak radiation temperature for the transitions at 47 and 48 GHz is about 15 mK, which yields an upper limit of $N \sim 2 \times 10^{12} \text{ cm}^{-2}$ in IRC +10216 for the column density of C_8H^- —about 2.5 times lower than the column density of neutral C_8H (Cernicharo & Guélin 1996). Chemical models predict that the column density of C_8H^- may be as high as 25% that of C_8H in IRC +10216 (Millar et al. 2000), so C_8H^- might be detectable with a two- to threefold deeper integration than that required for C_6H^- . Following our recent detection of C_6H^- in TMC-1, it may now be possible to detect C_8H^- in this source. Examination of the recent 45 m Nobeyama survey between 8.8 and 50 GHz (Kaifu et al. 2004), reveals no lines of C_8H^- , but C_8H and C_6H^- are not observed in this survey and were found only after deep

searches at precise frequencies. We estimate that lines of C_8H^- near 19 GHz should be about 10 mK on the assumption that the abundance of C_8H^- is 2.5% that of neutral C_8H (the same ratio as C_6H^-/C_6H ; McCarthy et al. 2006)—sufficient to be detected with the 100 m Green Bank Telescope in a deep search at the laboratory rest frequencies.

In conclusion, the present work provides the spectroscopic data required to search for the two anions C_4H^- and C_8H^- in astronomical sources. Because of our recent detection of the closely related C_6H^- anion, they are likely candidates for astronomical detection. Both anions have been detected with high signal-to-noise ratios in the laboratory, suggesting that other anions may be found with our present instrumentation. Of particular interest are those with high stability, i.e., high binding energies, large dipole

moments, and simple rotational spectra. Good candidates include the cyano compounds $C_{2n+1}N^-$, which are the isoelectronic nitrogen analogs to the hydrocarbon chains $C_{2n}H^-$, and the $H_2C_{2n}N^-$ and $H_2C_{2n+1}H^-$ anions.

We thank J. F. Stanton for guidance with the quantum calculations, E. S. Palmer for assistance with microwave electronics, and K. Higgins for the use of his workstations. F. T. acknowledges the University of Bologna for funding under the “Programma Marco Polo” scheme. This work is supported by National Science Foundation Grant CHE-0353693; additional support is provided by the Robert A. Welch Foundation through a grant to J. F. Stanton at the University of Texas.

REFERENCES

- Bell, M. B., Matthews, H. E., & Sears, T. J. 1983, *A&A*, 127, 241
Botschwina, P. 2000, in 55th Int. Symp. on Molecular Spectroscopy (Columbus: Ohio State Univ.), TC06
Cernicharo, J., & Guélin, M. 1996, *A&A*, 309, L27
Cernicharo, J., Guélin, M., & Kahane, C. 2000, *A&AS*, 142, 181
Gottlieb, C. A., Gottlieb, E. W., Thaddeus, P., & Kawamura, H. 1983, *ApJ*, 275, 916
Gottlieb, C. A., Myers, P. C., & Thaddeus, P. 2003, *ApJ*, 588, 655
Guélin, M., Mezaoui, A., & Friberg, P. 1982, *A&A*, 109, 23
Kaifu, N., et al. 2004, *PASJ*, 56, 69
Kawaguchi, K., Kasai, Y., Ishikawa, S.-I., & Kaifu, N. 1995, *PASJ*, 47, 853
McCarthy, M. C., Chen, W., Apponi, A. J., Gottlieb, C. A., & Thaddeus, P. 1999, *ApJ*, 520, 158
McCarthy, M. C., Chen, W., Travers, M. J., & Thaddeus, P. 2000, *ApJS*, 129, 611
McCarthy, M. C., Gottlieb, C. A., Gupta, H., & Thaddeus, P. 2006, *ApJ*, 652, L141
McCarthy, M. C., Travers, M. J., Kovács, A., Gottlieb, C. A., & Thaddeus, P. 1996, *A&A*, 309, L31
Millar, T. J., Herbst, E., & Bettens, R. P. A. 2000, *MNRAS*, 316, 195
Pachkov, M., Pino, T., Tulej, M., Guethe, F., Tikhomirov, K., & Maier, J. P. 2003, *Mol. Phys.*, 101, 583
Pan, L., Rao, B. K., Gupta, A. K., Das, G. P., & Ayyub, P. 2003, *J. Chem. Phys.*, 119, 7705
Pino, T., Tulej, M., Güthe, F., Pachkov, M., & Maier, J. P. 2002, *J. Chem. Phys.*, 116, 6126
Stanton, J. F., Gauss, J., Watts, J. D., Lauderdale, W. J., & Bartlett, R. J. 1992, *Int. J. Quantum Chem. Symp.*, 26, 879
Taylor, T. R., Xu, C., & Neumark, D. M. 1998, *J. Chem. Phys.*, 108, 10018
Terzieva, R., & Herbst, E. 2000, *Int. J. Mass. Spectrom. Ion Processes*, 201, 135
Woon, D. E. 1995, *Chem. Phys. Lett.*, 244, 45